Influence of Cu Substitution on the Structure and Magnetic Properties of Partially Crystallized $Fe_{62-x}Co_{10}Y_8Me_xB_{20}$ Alloys

KONRAD GRUSZKA[1]*, MARCIN NABIALEK[1], MICHAL SZOTA[2]

[1]Institute of Physics, Faculty of Production Engineering and Materials Technology, Czestochowa University of Technology, 19 Armii Krajowej Str., 42-200 Czestochowa, Poland

[2]Institute of Materials Science and Engineering. Department of Materials Processing Technology and Applied Physics, Czestochowa University of Technology, 19 Armii Krajowej Str., 42-200 Czestochowa

The paper presents results of structural and magnetic properties investigation of partially crystallized Fe62Co10Y8B20 and Fe61Co10Y8Cu1B20 alloys. Multicomponent bulk amorphous alloys exhibit a significant sensitivity to the composition changes. Even a small quantitative element substitution in composition of the initial alloy may lead to substantial changes in its various properties. Samples in form of thin plates were obtained by radial cooling method resulting in a complete amorphous structure material. Then, the one-step controlled heat treatment process led to partial crystallization of the sample causing the coexistence of amorphous matrix and embedded nanocrystalline phases. As shown in article, amorphous matrix has a noticeable influence on nano-sized grains resulting in a deformation of primary cell structure. Isothermal annealing process also had an impact on the magnetic properties of obtained samples, which was examined by the vibrating sample magnetometer (VSM).

Keywords: Amorphous materials, metals and alloys, Bulk metallic glasses, Computed tomography, microstructure, X-ray diffraction

Iron based soft magnetic alloys with various metallic and non-metallic additions are of great interest due to excellent properties exhibited by these materials [1-3]. The main application of these materials are located in cores of modern electrical devices like chokes, coils and high power transformers, where they work under varying magnetic field. For this reason, they must meet special requirements, that will allow to reduce magnetic reversal losses, giving a rise to efficiency.

Typically for the production of a material having good soft magnetic properties [4-7] especially low coercivity and low core losses, the rapid solidification of melted alloy technique is used [8]. This results in obtaining of material that is characterized by lack of long range order and which has good magnetic homogeneity. This homogeneity is a one of main contributions to the excellent soft magnetic properties. It is well known, that amorphous materials exhibit low magnetic anisotropy constant, which indicate that less external energy is needed to rotate the magnetic vectors. This is a consequence of random (or heavily disordered) nature of the atomic arrangement in amorphous solids [9]. Additionally, differently than for crystalline materials amorphous structure tends to random distribution of the orientation of atomic magnetic vectors, which leads to lack of magnetic easy axis. Another important aspect of modern soft magnetic materials is to minimize the coercivity field, which essentially depends on the anchoring of domain walls during magnetization process. Anchoring of the walls takes place in a similar manner as in crystalline materials, where mainly responsible for this process are structural defects and inhomogeneities [10]. Therefore, defects should be eliminated by proper thermal treatment.

Amorphous soft magnetic materials with low core losses and low coercivity suffer only for low magnetic saturation. In order to improve this parameter the nanocrystallization process is introduced. In this way, magnetic saturation can be enhanced, while still leaving other important parameters at fairly high level.

In this paper we introduce a small 1% Cu addition at the expense of Fe, while performing a heat treatment leading to nanocrystallization of the studied samples. The 1% of Cu addition should act as destabilizer lowering the crystallization temperature and activation energy of the first stage of crystallization [11, 12].

Experimental part

Material and procedures

In this work two samples of $Fe_{62}Co_{10}Y_8B_{20}$ and $Fe_{61}Co_{10}Y_8Cu_1B_{20}$ compositions were prepared from high purity components (Fe - 99.95%, 99.99% - remaining ingredients). For the preparation a two step procedure was used. In a first step all ingredients were melted and freely solidified together in a plasma arc furnace under protective atmosphere of argon. Resulting ingots were melted several times to provide a good mixing of constituents and uniform samples homogeneity. Then, in a second step ingots were melted by induction furnace also under protective atmosphere of argon, and then injected into copper water-cooled mold. Thus prepared amorphous samples were examined by XRD diffractometer (Bruker D8 Advance, Cu-Kα, 1.54 Å), VSM sample magnetometer (LakeShore, model 7301) and then subjected to thermal annealing in 927 K for 900 s. The heat treatment parameters were selected based on DSC experiment so as to heat the samples slightly below crystallization temperature. Quantitative Rietveld phase refinement was performed using Fullprof software. The fit was performed using: scale factor, unit cell and additional background parameters. A shifted background polynomial with 5 parameters was used to refine the background signals. A pseudo-Voigt function described the peak shapes.

Results and discussions

Figure 1 shows XRD patterns taken for samples $Fe_{62}Co_{10}Y_8B_{20}$ (1.A) and $Fe_{61}Co_{10}Y_8Cu_1B_{20}$ (1.B) in state after solidification within the 2θ angle from 30° up to 100° with a 0.02° step size. As can be seen patterns consists of one broad diffuse maximum localized in range from about 35

* *email: kgruszka@wip.pcz.pl*

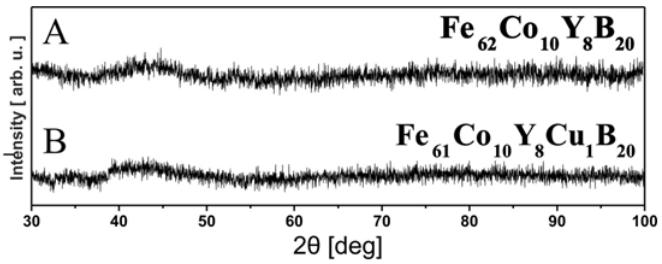

Fig. 1. XRD patterns for samples $Fe_{62}Co_{10}Y_8B_{20}$ (A) and $Fe_{61}Co_{10}Y_8Cu_1B_{20}$ (B) in state after solidification1

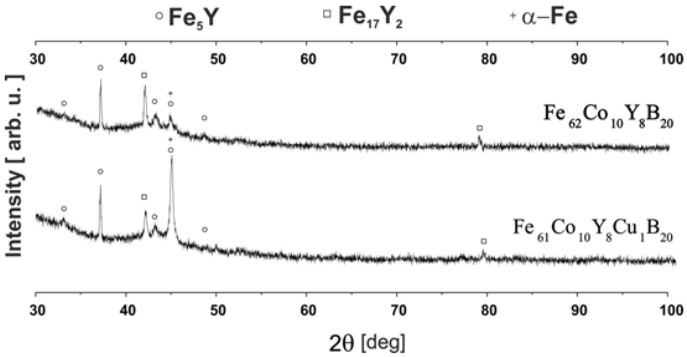

Fig. 2. XRD patterns for samples $Fe_{62}Co_{10}Y_8B_{20}$ (top) and $Fe_{61}Co_{10}Y_8Cu_1B_{20}$ (bottom) in state after isothermal annealing for 900 s in 927 K

to 50°. The lack of sharp narrow peaks indicates that there is no long range order present in studied samples.

XRD patterns of samples after isothermal annealing in 927 K for 900 s are shown in figure 2.

As can be seen in figure 2 a relatively narrow peaks with different intensities appeared in coexistence with amorphous blurred halo. The presence of peaks in the diffraction patterns shows the emergence of X-ray reflecting planes, which are associated with the presence of long-range order. It means, that structure of the sample consists of crystalline phases together with amorphous phase. In fact, that kind of XRD pattern is characteristic to nanocrystallites embedded in amorphous matrix. Individual peaks were identified and attributed to the three phases α-Fe, Fe_5Y and $Fe_{17}Y_2$ using as reference PDF2 database. In each case, the peak positions (derived from the individual phases) are slightly shifted relative to the pure crystalline phases. As the stresses within the amorphous matrix are significant, they affect the embedded grains. Next, the average grain size was calculated using modified Sherrer equation [13]:

$$\beta^2 / tg^2\theta = \lambda / D\left(\beta / tg\theta \sin\theta\right) + 16e^2 \quad (1)$$

where β is the function:

$$\beta = B\left(1 - b^2 / B^2\right) \quad (2)$$

and: e - is the factor of lattice deformation, D – represents the grain size (perpendicular to *hkl*), θ - is the Bragg angle, B - is the width of reflex of the studied sample, b - is the width of the reference sample and λ - is the radiation wavelength.

The data from calculation of average grain size are summarized in table 1.

Table 1
AVERAGE GRAIN SIZE CALCULATED BY MODIFIED SHERRER EQUATION

Phase	$Fe_{62}Co_{10}Y_8B_{20}$	$Fe_{61}Co_{10}Y_8Cu_1B_{20}$
$Fe_{17}Y_2$	9 nm	8 nm
Fe_5Y	40 nm	44 nm
α-Fe	38 nm	61 nm

As can be seen, in general, grain size distribution is similar in both cases with the exception of α-Fe phase in $Fe_{61}Co_{10}Y_8Cu_1B_{20}$ where the grain size is nearly twice as bigger.

This is also visible in XRD pattern where the intensity of the peak near 45° is higher in the case of sample with Cu addition. This increase in intensity can be also related to increase in quantity of α-Fe phase. To check this possibility a Rietveld refinement was performed and data obtained from share analysis are summarized in table 2.

Table 2
MUTUAL SHARE OF CRYSTALLINE PHASES

Sample	Phase		
	α-Fe (%)	Fe_5Y (%)	$Fe_{17}Y_2$ (%)
$Fe_{62}Co_{10}Y_8B_{20}$	20.21	52.32	27.37
$Fe_{61}Co_{10}Y_8Cu_1B_{20}$	67.91	28.49	3.60

The mutual share of identified phases differ significantly between studied samples. Despite the same conditions of annealing process it is clear, that crystallization dynamics are different leading to different mutual share of crystalline phases.

In order to determine the influence of the amorphous matrix on the embedded grains a refinement of unit cell was carried out and the results are shown in table 3.

The analysis of data contained in table 2 reveals that in contrast to $Fe_{62}Co_{10}Y_8B_{20}$ sample, in $Fe_{61}Co_{10}Y_8Cu_1B_{20}$ there are no significant changes of elementary cell parameters. Also, in both samples the α-Fe phase practically didn't changed.

Next, the influence of Cu addition on the magnetic properties were examined by measurements of static hysteresis loops for both samples before and after isothermal annealing process (figs. 3 and 4).

Sample		Phase				
		α-Fe	Fe_5Y		$Fe_{17}Y_2$	
Lattice parameter		*a* (Å)	*a* (Å)	*c* (Å)	*a* (Å)	*c* (Å)
Old		2.8600	4.9700	3.9100	8.4580	8.0070
Calc.	$Fe_{62}Co_{10}Y_8B_{20}$	2.8600	5.0700	4.0005	8.4161	7.9086
	$Fe_{61}Co_{10}Y_8Cu_1B_{20}$	2.8604	4.9698	3.9103	8.4577	8.0066

Table 3
RIETVELD REFINEMENT OF ELEMENTARY CELL PARAMETERS FOR ISOTHERMALLY ANNEALED SAMPLES

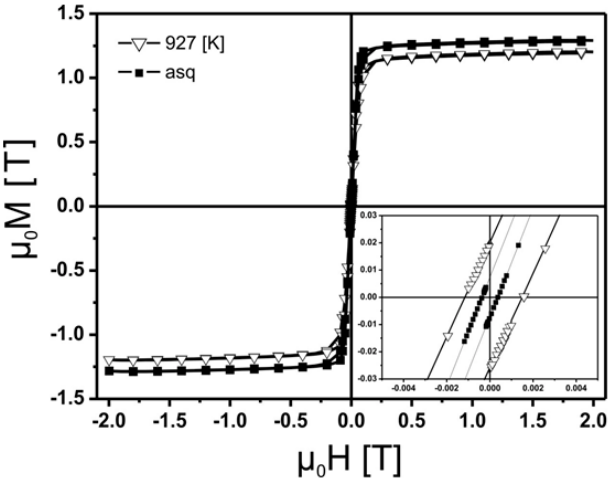

Fig. 3. Static hysteresis loops measured for $Fe_{62}Co_{10}Y_8B_{20}$ sample

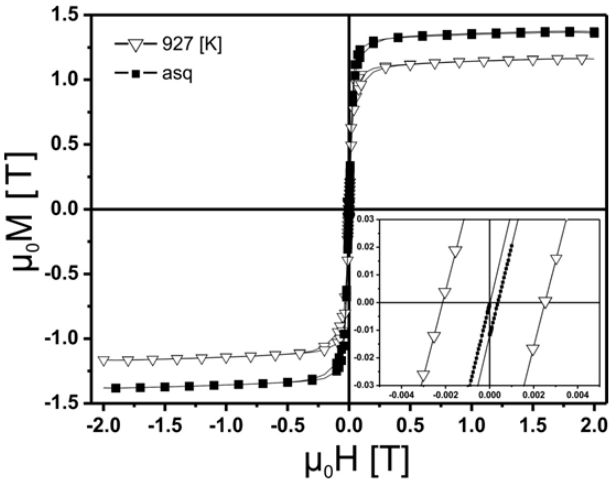

Fig. 4. Static hysteresis loops measured for $Fe_{61}Co_{10}Y_8Cu_1B_{20}$ sample

The data obtained from analysis of static hysteresis loops are summarized in table 4.

As can be seen in table 4, both samples significantly worsen their soft magnetic parameters.

The isothermal annealing process lead to nano-crystallization. Grains significantly influenced the magnetic parameters of investigated alloys giving a rise both to magnetic saturation and coercivity. Crystalline phases that have arisen in the samples with the exception of α-Fe are considered as metastable semi-hard magnetic phases. According to the literature, seeds of $Fe_{17}Y_2$ and Fe_5Y phase nucleate at relatively high temperature [14]. The decomposition of γ-Fe phase at 1173 K enables growth of Fe_5Y and then with the decrease in temperature it competes with emerging $Fe_{17}Y_2$ and α-Fe phases. $Fe_{61}Co_{10}Y_8Cu_1B_{20}$ sample initially had better magnetic parameters which indicates that a small addition of Cu has a positive effect on this material in a amorphous state. At the same time this addition apparently made possible for grains in the material to grow larger [11, 12]. The deterioration of coercivity field in all cases is related to relative big size of grains which are becoming anchoring sites and additionally introducing magnetic anisotropy [15-17]. Despite the fact that in the $Fe_{61}Co_{10}Y_8Cu_1B_{20}$ sample there is a much bigger share of soft magnetic α-Fe phase, simultaneously the grains size of this phase are largest, deteriorating magnetic characteristics. The influence of amorphous matrix on nanometric grains in case of sample with Cu addition is negligible, probably due to their relative large size. In the case of $Fe_{62}Co_{10}Y_8B_{20}$ sample, the matrix has noticeable influence on elementary cell parameters.

Table 4
DATA OBTAINED FROM ANALYSIS OF HYSTERESIS LOOPS

State	Sample	Saturation [T]	Coercivity [A/m]
ASQ	$Fe_{62}Co_{10}Y_8B_{20}$	1.27	289
927	$Fe_{62}Co_{10}Y_8B_{20}$	1.20	1057
ASQ	$Fe_{61}Co_{10}Y_8Cu_1B_{20}$	1.36	139
927	$Fe_{61}Co_{10}Y_8Cu_1B_{20}$	1.16	1550

Conclusions

By the use of radial cooling method an amorphous samples were obtained and then subjected to a nanocrystallization process. This resulted in grains of nanometric sizes, where the average size of largest exceeded 60 nm. Cu addition changed crystallization dynamics resulting in different mutual share of the crystalline phases and their grains sizes. The emergence of semi-hard phases considerably worsen soft magnetic properties.

References

1.PIETRUSIEWICZ P, B£OCH K., NABIALEK M., WALTERS S., Acta Phys. Pol. A. Vol **127,** 2011, p. 397-399
2.NABIALEK M, DOŒPIA£ M., SZOTA M., PIETRUSIEWICZ, JÊDRYKA J., J. Alloy. Compd. **509** 2011 p. 3382-3386
3.GRUSZKA K., NABIA£EK M, B£OCH K., Arch. Metall. Mater., Vol. **61,** 2016, No 2, p. 499–502
4.POIANA, M., DOBROMIR, M., SANDU, A.V., GEORGESCU, V., J. Superconductivity Novel Magn., **25**(7), 2012, p. 2377.
5.POIANA, M., VLAD, L.,PASCARIU, P., SANDU, A.V., NICA, V., GEORGESCU, V., Optoelectron Adv Mater-RC, **6**(3-4), 2012, p. 434.
6.NABIALEK M., PIETRUSIEWICZ, P., SZOTA, M., ABDULLAH, M.M.A.B., SANDU, A.V., Rev. Chim. (Bucharest), **68**, no. 1, 2017, p. 22.
7.BLOCH, K., NABIALEK, M., SZOTA, M., Rev. Chim. (Bucharest), **68**, no. 1, 2017, p. 18.
8.LOTOFOLLAHI Z., GARCIA-ARRIBAS A., AMIRABADIZADEH A., ORUE I., KURLYANDASKAYA G.V., Journal of Alloys and Compounds, Volume **693**, 2017, p. 767-776
9.ZAMORA J., BETANCOURT I., Journal of Magnetism and Magnetic Materials, Vol **428**, 2017, p. 165-170
10.GRUSZKA K, Materiali in Tehnologije **50**(5), 2016, p. 707-718
11.MAKINO A., KUBOTA T., YUBUTA K., INOUE A., FeSiBPsi nanocrystalline soft magnetic alloys with high bS of 1.9 tesla produced by crystallizing hetro-amorphous phase. Materials Transactions, 2009.
12.SUZUKI K., MAKINO A., INOUE A., MASUMOTO T., J. Appl. Phys. 70, 1991 p. 6232
13.E. MITTEMEIJER, U. WELZEL IN: E. MITTEMEIJER, U. WELZEL (EDS.), Modern Diffraction Methods, VCH, Weinheim (2013) 87. DOI: 10.1002/9783527649884.fmatter
14.MIHALKOVIC M., WIDOM M., MRS Symposia Proceedings, edited by E. Belin (Materials Research Society, Pittsburgh, 2003), Vol. 805, p.83; Phys. Rev. Lett. 93, 095507 (2004)
15.HERZER G. Modern soft magnets: Amorphous and nanocrystalline materials. Vol **61**(3), 2013, p. 718–734
16.HERZER G. Nanocrystalline soft magnetic materials. G Herzer Journal of Magnetism and Magnetic Materials **112**, 1992, p. 258-262
17.KULIK T., Nanokrystaliczne materialy magnetycznie miêkkie otrzymywane przez krystalizacje szkie metalicznych, Oficyna wydawnicza Politechniki Warszawskiej, (1998)

Manuscript received: 23.12.2016